EVALUATION OF THE SUB-PIXEL PERFORMANCE OF ANOMALY DETECTORS

D. Borghys, C. Perneel
Royal Military Academy
Signal & Image Centre
Brussels, Belgium

V. Achard
ONERA
French Aerospace Lab
Toulouse, France

I. Kasen
Norwegian Defence
Research Establishment (FFI)
Kjeller, Norway

ABSTRACT

Anomaly detection in hyperspectral data has received much attention for various applications and is especially important for defense and security applications. Anomaly detection detects pixels in the hyperspectral data cube whose spectra differ significantly from the background spectra. Most existing methods estimate the spectra of the (local or global) background and then detect anomalies as pixels with a large spectral distance w.r.t. the determined background spectra. Many types of anomaly detectors have been proposed in literature. The most well-known anomaly detector is the RX detector that calculates the Mahalanobis distance between the pixel under test and the background. This paper investigates the sub-pixel detection performance of two classes of anomaly detectors: the family of RX-based detectors and the segmentation-based anomaly detectors. Representative examples of each class are selected and results obtained on three different datacubes are analyzed.

Index Terms— Anomaly detection, sub-pixel detection, hyperspectral data

1. INTRODUCTION

Many types of anomaly detectors (ADs) have been proposed in literature [1]. The benchmark anomaly detector is the Reed-Xiaoli (RX) algorithm [2]. Different variations of this method have been proposed in literature [3, 4, 5, 6, 7]. This paper investigates the sub-pixel detection capabilities of two classes of anomaly detectors by comparing their results on a set of three datacubes with artificially inserted sub-pixel anomalies with varying mixing ratio. The first class of examined detectors is the family of linear RX-based anomaly detectors. The second class consists of segmentation-based anomaly detection methods.

2. DATASET

The analysis was performed on a set of 3 hypercubes acquired by 2 different airborne sensors. Each image is a part of a real hyperspectral image in which anomalies are inserted artificially by linearly mixing the spectra of a green paint or fabric, taken from another part of the image, with the original background pixel. The mixing ratio of the anomaly varies from 100% (full-pixel) to 10 or 5%. Fig. 1 shows RGB composites of each of the examined datacubes with the full-pixel targets. Table 1 presents the main characteristics of the dataset. The first column is the name by which the scenes will be referred further in this paper. As can be seen from the figure HAR and CAM present a more structured background than OSL.

3. ANOMALY DETECTION METHODS

3.1. RX-based anomaly detectors

The RX detector [2] is a standard in anomaly detection. Basically the RX detector calculates the Mahalanobis distance between the current pixel and the background:

$$D_{RX} = (\overline{r} - \overline{\mu}_B)^t \overline{\overline{C}}_B^{-1} (\overline{r} - \overline{\mu}_B)$$

$\overline{\overline{C}}_B$ and $\overline{\mu}_B$ are respectively the sample spectral covariance matrix and the spectral mean of the background pixels; $\overline{r}$ is the spectrum of the current pixel. Many different implementations of the RX detector have been proposed in literature. They differ in the way the background covariance matrix and background mean is defined and estimated and also in the manner in which the inverse of the covariance matrix is implemented.

- **Global RX (GRX)** In this paper the GRX detector estimates the covariance matrix and mean of the background using all pixels of the image and all spectral bands. GRX thus has no parameters.

- **Complementary Subspace Detector (CSD)** In the CSD the highest variance PCs are used to define the background subspace and the others (the complementary subspace) the target subspace [4]. The pixel under test (PUT) is then projected on the two subspaces and the anomaly detector is the difference of the projection onto the target subspace and the background subspace. Spectral whitening is applied as pre-processing step.

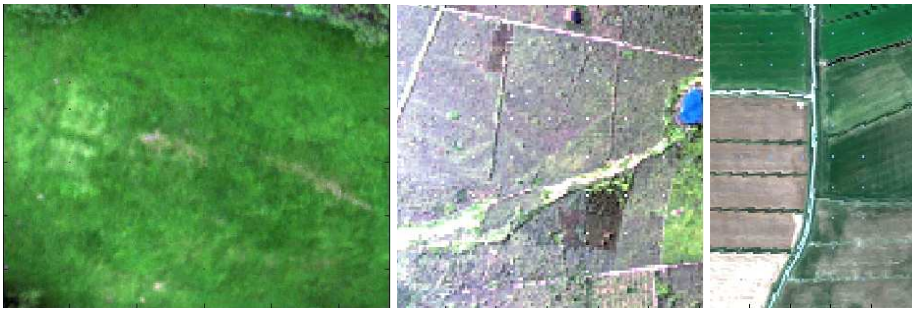

Fig. 1. RGB composite of the original datacubes. From left to right: OSL, HAR, CAM

Name	Site	Sensor name	# bands	Waveband (μm)	Image Size	# target pixels	Scene Description	Type of anomalies
OSL	Oslo (No)	HySpex	80	0.41-0.98	286x287	81	Park near Oslo	green fabric
HAR	Hartheim (Ge)	Hymap	118	0.44-2.45	121x121	49	Agricultural area	green paint
CAM	Camargue (Fr)	Hymap	119	0.44-2.45	150x100	45	Agricultural area	green paint

Table 1. Overview of the dataset

- **Sub-space RX (SSRX)** In this paper SSRX is the GRX applied after PCA and the background statistics are determined on a limited number of PCA bands. Usually the first PCs are discarded in SSRX.

- **RX after orthogonal subspace projection (OSPRX)** In OSPRX the background is defined by the first components of a Singular Value Decomposition. These first components define the background subspace and the data are projected onto the orthogonal subspace before applying the RX detector [1].

- **Partialling Out RX detector (PORX)** [5] In this method the effect of the clutter in a pixel is partialled out component-wise by predicting each of its spectral components as a linear combination of its high-variance principal components. The detector applies then a Mahalanobis distance on the residual.

- **Local RX (LRX)** In this case the covariance matrix and mean is determined locally in a window around the PUT. A double sliding window is used: A guard window and an outer window are defined and the background statistics are determined using the pixels between the two. The covariance matrix is regularized using diagonal loading before inversion [8]. The scale factor for the diagonal loading used here is the median of the eigenvalues of the covariance matrix calculated on the complete image. Parameters of LRX are the guard and outer window sizes (GWS, OWS).

- **Quasi-local RX (QLRX)** In quasi-local RX the global covariance matrix is decomposed using eigenvector/eigenvalue decomposition [6]: $\overline{\overline{C}}_B = \overline{U}\ \overline{\overline{\Lambda}}\ \overline{U}^T$. The eigenvectors are kept in the RX, but the eigenvalues are replaced by the maximum of the local variance and the global eigenvalue. This means that the score of the detector will be lower at locations of the image with high variance (e.g. edges) than in more homogeneous areas. Spectral statistical standardization is applied as pre-processing step. The local variance is determined in a double sliding window. Parameters are OWS and GWS.

3.2. Segmentation-based anomaly detectors - SBAD

- **Class-Conditional RX (CCRX)** Although CCRX is also an RX-based method, it is cataloged here under SBAD because it is also based on image segmentation. In CCRX the image is first segmented, the global covariance matrix and mean within each class is determined. The Mahalanobis distance between the PUT and each of the classes is calculated. The final result is the minimum of these distances. In the current paper K-means clustering is used and the parameter of the method is the number of classes (NC) used in the clustering.

- **Method based on Multi-normal mixture models (MMM)** A Stochastic Expectation Maximization (SEM) algorithm [9] is used for fitting a multi-normal mixture to the image for describing the background. A 7-component mixture is used. The anomaly detector detects pixels having a low probability according to the estimated model. The MMM was applied after spectral

binning.

- **Two-level endmember selection method (TLES)** The principle of this method [10] is the following: a small scanning window (typically 50×50 pixels) runs over the image and at each position of the window the principal background spectra are determined using a segmentation method based on end-member selection. Endmembers that correspond to a minimum percentage (MP) of the image tile are stored. At the end of the process an endmember selection is again applied on the stored endmembers and linear unmixing is applied on the image. Anomalies correspond to pixels with a large residue after unmixing. The parameters of the method are the number of endmembers in the first and last stage and MP.

- **Method based on a Self-Organizing Map (SOM)** A trained SOM is considered as a representation of the background classes in the scene. Anomalies are determined by computing the spectral distances of the pixels from the SOM units [11]. The SOM was applied on the first three PCA components and run using a square map consisting of NsxNs hexagonal cells. It was optimized sequentially and its only free parameter is Ns.

4. RESULTS AND DISCUSSION

The evaluation of the results is based on the receiver/operator curves (RoC curves). These are curves that plot the probability of detection (Pd) versus the probability of false targets (Pf). The evaluation measure is the area under the curve (AUC); the integral of the curve between Pf=0 and Pf=1. The integral is calculated using a logarithmic scale for Pf. This leads to much lower values than when a linear AUC is calculated, but allows to distinguish to a much larger extent between behaviours at the low Pf range. For all the algorithms, parameters were varied within a reasonable range and the shown results are the best results obtained for the algorithm.

The influence of prior spectral whitening was also investigated. Only for GRX results are significantly influenced by spectral whitening: for OSL the best results for GRX are obtained without whitening, while for HAR and CAM the results with whitening are much better.

Fig. 2 presents the logarithmic areas under the RoC curve (Logarithmic AUC) for the different detectors versus the mixing ratio for OSL. LRX gives, by a good margin, the best results. At mixing ratios of 5% and 10% the CSD and PORX give the second best results. From a MR=25%, the MMM gives the second best results.

Fig. 3 shows the RoC curves for the CAM and HAR scenes, for the lowest mixing ratio (MR=10%). In both cases MMM gives a perfect detection (AUC=1). LRX give comparable results (AUC=1 for CAM and slightly lower for HAR). OSPRX and QLRX give the next best, and also very good, results in both datasets. In all datasets TLES and SOM give the least good results, significantly less good than GRX.

The preprocessing (e.g. PCA, spectral binning) applied for some of the algorithms induces ”hidden” parameters (number of PCs kept/discarded, number of spectral bands) that can have a significant impact on the detection performance. This point will be investigated in further work.

5. CONCLUSIONS

This paper investigates the sub-pixel detection performance of linear RX-based anomaly detection methods and SBAD methods. The LRX gives very good results in all datasets. However, its results depend on the window sizes for outer window and guard window. In the datasets with a structured background the MMM detector gives the best results. The MMM also give very good results in the dataset with a homogeneous background. It seems, however, as if the MMM is not particularly well suited for detection of the smallest target fractions/lowest target contrasts. From the global RX-based methods OSPRX seems to give the best results. In a structured background QLRX also gives very good results. The results of the TLES and SOM detectors are significantly less good than those of GRX, these methods thus seem not well adapted for sub-pixel detection. The results are obtained on a limited data set. However, we find clear consistency in the results across different scenes recorded with different sensors, indicating that the results have a fair degree of generality.

6. ACKNOWLEDGMENTS

The OSL dataset was provided by the Norwegian Defence Research Establishment (FFI). The HAR scene is the courtesy of P. Wurteisen, European Space Agency, and the CAM image was provided by DLR. The authors thank S. Rotman and N. Gorelik from the Dept. of Elec. and Computer Eng. of the Ben-Gurion University of the Negev for applying their QLRX method on the HAR and CAM scenes.

7. REFERENCES

[1] Matteoli, M. Diani, and G. Corsini, “A tutorial overview of anomaly detection in hyperspectral imagery,” *IEEE A&S Systems Magazine, Part3: Tutorials*, vol. 21, no. 3, June 2010.

[2] I.S. Reed and X. Yu, “Adaptive multiband cfar detection of an optical pattern with unknown spectral distribution,” *IEEE ASSP*, vol. 38, no. 10, pp. 1760–1770, Oct 1990.

[3] D.W.J. Stein, S.G Beaven, L.E. Hoff, E.M. Winter, A.P. Schaum, and A.D. Stocker, “Anomaly detection from hyperspectral imagery,” *IEEE Signal Proc. Mag.*, vol. 38, pp. 58–69, Jan 2002.

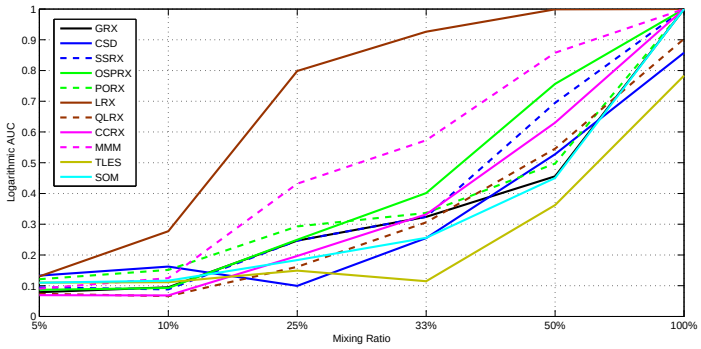

Fig. 2. Logarithmic AUCs versus the mixing ratio for the different detectors for the OSL dataset

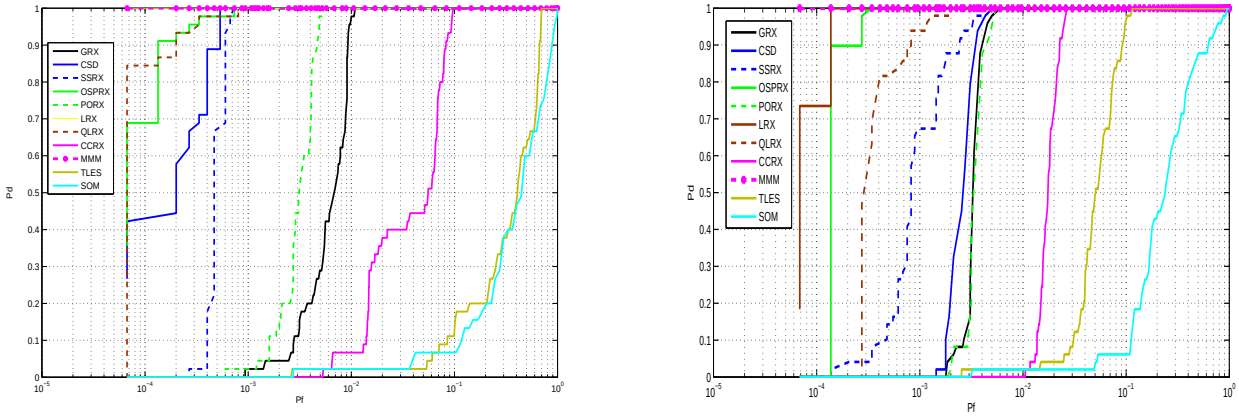

Fig. 3. RoC curves for the different detectors for CAM(left)and HAR(right); both at 10% mixing ratio. Note that the LRX result for CAM10 is equal to the MMM result, and hence not visible in the plot.

[4] A. Schaum, "Hyperspectral anomaly detection: Beyond rx," in *Proc. SPIE Algorithms and Technologies for Multispectral, Hyperspectral and Ultraspectral Imagery XII*, 2007, vol. 6565.

[5] E. Lo and A. Schaum, "A hyperspectral anomaly detector based on partialling out a clutter subspace," in *Proc. SPIE Algorithms and Technologies for Multispectral, Hyperspectral and Ultraspectral Imagery XV*, 2009, vol. 7334.

[6] C.E. Caefer, J. Silverman, O. Orthal, D. Antonelli, Y. Sharoni, and S.R. Rotman, "Improved covariance matrices for point target detection in hyperspectral data," *Optical Engineering*, vol. 47, no. 7, July 2008.

[7] H. Kwon and N.M. Nasrabadi, "Kernel rx-algorithm: A nonlinear anomaly detector for hyperspectral imagery," *IEEE-TGRS*, vol. 43, no. 2, pp. 388–397, Feb 2005.

[8] S. Matteoli, M. Diani, and G. Corsini, "Different approaches for improved covariance matrix estimation in hyperspectral anomaly detection," in *Proc. Annual Meeting*. Italian National Telecommunications and Information Theory Group - GTTI, 2009.

[9] P. Masson and W. Pieczynski, "Sem algorithm and unsupervised segmentation of satellite images," *IEEE-TGRS*, vol. 31, no. 3, pp. 618–633, Mar 1993.

[10] D. Borghys, E. Truyen, M. Shimoni, and C. Perneel, "Anomaly detection in hyperspectral images of complex scenes.," in *Proc. 29th Earsel Symposium*, Chania, June 2009.

[11] O. Duran and M. Petrou, "Spectral unmixing with negative and superunity abundances for subpixel anomaly detection," *IEEE-GRSL*, vol. 6, no. 1, pp. 152–156, Jan 2009.